Anal. Chem. **2002,** *74,* 1718−1723

Technical Notes

Fabrication of an Optoelectrochemical Microring Array

Sabine Szunerits and David R. Walt*

The Max Tishler Laboratory for Organic Chemistry, Department of Chemistry, Tufts University, Medford, Massachusetts, 02155

In this paper, we describe a novel approach for fabricating an optoelectrochemical microring array. The array was fabricated by coating individual optical fibers of 25-μm diameter with a 1-μm layer of gold nanoparticles via electroless gold deposition. A SAM layer around the individual gold-coated imaging fibers prevented electrical contact with neighboring ring electrodes. To achieve better mechanical stability and to make the device more practical, the electrode/fiber bundle comprising ~600 individual gold-coated optical fibers was dipped into epoxy. By polishing the ends of such a device, a ring microelectrode array comprising 600 individual and insulated ring electrodes was formed. To limit diffusional overlap of current, only 20−30% of the microring fiber/electrodes were wired. The inner diameter of the ring electrode is fixed by the diameter of the individual optical fibers (25 μm), while the outer radius is determined by the thickness of the deposited gold. The array was characterized using ferrocyanide in aqueous solution as a model electroactive species to demonstrate that this microelectrode array format exhibits steady-state currents at short response times. In addition, cyclic voltammetry experiments were performed using conventional potentiostats due to the amplification of current inherent in the array format. Finally, electrochemiluminescence at the ring electrode array was demonstrated through the oxidation of Ru(bpy)$_3^{2+}$ in tri-*n*-propylamide in a pH 7 phosphate buffer solution, where the light generated was collected and detected via the fiber bundle.

Microelectrodes are gaining increased importance in electrochemical analysis and sensor technology as their small size leads to small faradaic currents, reduced *iR* drop, and steady-state diffusion currents.[1−3] Beside electrochemical devices, optical fibers and optical fiber bundles allowing simultaneous sensing and imaging have been used increasingly for a variety of different applications.[4−7] The idea of coupling both analytical methods via the fabrication of ring-shaped microelectrodes around optical fibers is not completely new, and these devices have been already used for photochemical microscopy,[8−10] in photochemical experiments,[11,12] and very recently in a SECM probe.[13] In this paper, we report the fabrication and electrochemical characterization of an optoelectrochemical array based on microrings. The advantage of using an electrochemical array over single ring-shaped microelectrodes around optical fibers is that, by combining several individual microelectrodes into an array, higher currents may be achieved without losing the benefits gained from miniaturization. Such arrays possess all the advantages of microelectrodes, including rapid response time, steady-state diffusion layer, and small *iR* drop, while providing higher currents. These advantages of microelectrode arrays can be combined with the imaging properties of optical fiber bundles. The literature on methods for fabricating assemblies is steadily increasing and range from micro-[14] and photolithography[15] to electroless deposition of gold into nanoporous membranes.[16−19] Randomly ordered arrays have been formed by embedding micrometer-sized conducting substances, such as carbon fibers, in an insulating material to provide a robust and repolishable material.[20−22] The number of electrodes in an array can vary considerably. While Evans[21] discussed microelectrode arrays comprising 17 or 29 disks of 25- and 10-μm diameters, respectively, the array described by Jimbo,[15] fabricated through photolithography, contains 64 electrodes of

(1) *Ultramicroelectrodes*; Fleischmann, M., Pons, S., Rolison, D. R., Schmidt, P. P., Eds.; Datatech Science: Morgantown, NC, 1987.
(2) Amatore, C. In *Physical Electrochemistry: Principles, Methods and Applications*; Rubinstein, I., Ed.; Marcel Dekker: New York, 1995; p 131
(3) Wightman, R. M.; Wipf, D. O. In *Electroanalytical Chemistry*; Bard, A. J., Ed.; Marcel Dekker: New York, 1989; Vol. 15, pp 267−353.
(4) Blum, L. J.; Gauthier, S. M.; Coulet, P. R. *Anal. Lett.* **1988**, *21*, 717.
(5) Luo, S.; Walt, D. R. *Anal. Chem.* **1989**, *61*, 1069.
(6) Walt, D. R. *Acc. Chem. Res.* **1988**, *31*, 267.
(7) Pantano, P.; Walt, D. R. *Anal. Chem.* **1995**, *67*, 481A.
(8) Casillas, N.; James, P.; Smyrl, W. H. *J. Electrochem. Soc.* **1995**, *142*, L16.
(9) James, P.; Casillas, N.; Smyrl, W. H. *J. Electrochem. Soc.* **1996**, *143*, 3853.
(10) Shi, G.; Garfias-Mesias, L. F.; Smyrl, W. H. *J. Electrochem. Soc.* **1998**, *145*, 2011.
(11) Kuhn, L. S.; Weber, A.; Weber, S. G. *Anal. Chem.* **1990**, *62*, 1631.
(12) Pennarun, G. I.; Boxall, C.; O'Hare, D. *Analyst* **1996**, *121*, 1779.
(13) Lee, Y.; Amemiya, S.; Bard, A. *J. Anal. Chem.* **2001**, *73*, 2261.
(14) Huber, C. A.; Huber, T. E.; Sadoqi, M.; Lubin, J. A.; Manalis, S.; Prater, C. B. *Science* **1994**, *263*, 800.
(15) Jimbo, Y.; Robinson, H. P. C. *Bioelectrochemsitry* **2001**, *51*, 107.
(16) Martin, C. R. *Science* **1994**, *266*, 1961.
(17) Menon, V. P.; Martin, C. R. *Anal. Chem.* **1995**, *67*, 1920.
(18) Jirage, K. B.; Hulteen, J. C.; Martin, C. R. *Science* **1997**, *278*, 655.
(19) Kobayashi, Y.; Martin, C. R. *Anal. Chem.* **1999**, *71*, 3665.
(20) Fletcher, S.; Horne, M. D. *Electrochem. Commun.* **1999**, *1*, 502.
(21) Strohben, W. E.; Smith, D. K.; Evans, D. H. *Anal. Chem.* **1990**, *62*, 1709.
(22) Nagale, M. P.; Fritsch, I. *Anal. Chem.* **1998**, *70*, 2908.

10.1021/ac010933t CCC: $22.00
Published on Web 02/23/2002

30 × 30 μm dimensions. Through mechanical assembly, arrays of 200−2000 carbon disks have been prepared, where only 20−40% of the electrodes in the assembly were active.[22]

We took advantage of two techniques, the electroless deposition of gold and the mechanical assembly of randomly ordered arrays to prepare ring-shaped microelectrodes and microelectrode arrays. We show that optical fibers coated with a layer of nanogold particles around the shaft and polished at the distal ends can be assembled into a ring microelectrode device that can be used for electrochemiluminescence (ECL) studies. The fabrication of such an optoelectrochemical array was based on electroless deposition of gold onto ∼600 individual optical fibers. When designing random assemblies of microelectrodes, it is critical to avoid diffusional interference between adjacent electrodes. The array was therefore designed in such a way so as to minimize the possibility of such interference by connecting only 20−30% of the fibers in the bundle. Furthermore, through the formation of a self-assembled thiol monolayer (SAM) on the gold around each individual fiber, we ensured each fiber was insulated from its neighbors. After the individual fibers were insulated with a SAM, they were embedded into an insulating epoxy to provide a mechanically stable and easily handled microarray assembly. The SAM deposition provided an expedient method for efficiently insulating the individual fibers. This assembly route also preserved the ability of the optical fibers to transmit light. Polishing the distal ends of this device resulted in the formation of microring electrodes immediately adjacent to the optical fiber. The electrochemical behavior of such a device in aqueous $Fe(CN)_6^{4+}$ solution will be described as well as a system using electrogenerated chemiluminescence with tris(2,2′-bypyridine)ruthenium(II) ($Ru(bpy)_3^{2+}$) in the presence of tri-*n*-propylamine (TPrA).

EXPERIMENTAL SECTION

Materials. Insulating epoxy (Araldite AM 136/Hy 994) was obtained from Ciba Geigy (East Lansing, MI). Conducting epoxy (Epo-Tek H20E) was purchased from Epoxy Technology (Billerica, MA). $SnCl_2$, tris(2,2′-bypyridyl)ruthenium(II) chloride hexahydrate, tri-*n*-propylamine, 11-mercapto-1-undecanol, trifluoroacetic acid, formaldehyde, H_2SO_4, $AgNO_3$, Na_2SO_3, H_2O_2, NH_4OH, methanol, ethanol, and nitric acid were purchased from Aldrich and used as received. A commercial gold-plating solution ($Na_3Au(SO_3)_2$, Oromerse SO Part B (5.67 g/100 mL), was obtained from Technic Inc. (Cranston, RI).

The optical fibers used for the construction of the array were raw glass fibers made of fused-silica glass purchased from Edmund Industrial Optics (Barrington, NJ). Each individual fiber had a 25-μm diameter and was cut to a length of ∼10 cm. Approximately 600 of these raw glass fibers were bundled together with the help of a 1-cm-long rubber tube acting as an O-ring. This bundling enabled easier handling of the individual fibers and allowed simultaneous modification of their glass surfaces. After gold deposition and insulation in a polymer, the array was polished with 30-, 15-, 3-, and 0.3-μm lapping films (General Fiber Optics, Fairfield, NJ) to expose the ring electrodes around the optical fibers.

Instrumentation. The potentiostat used was a PGSTAT 30 Autolab (Eco Chemie). All experiments were performed using a Ag/AgCl reference electrode. The counter electrode was a platinum wire. Solutions were purged with nitrogen. In all experiments a low-current amplifier and a Faraday cage were used (Bioanalytical Systems, model C2).

The instrumental setup for imaging and fluorescence measurements has been described in detail previously.[23] The array was fixed in a cell (V = 1 mL) containing the counter and the reference electrodes and mounted on the stage of the imaging system. No excitation wavelength was used as $Ru(bpy)_3^{2+}$ was excited electrochemically. The ECL returning through the optoelectrochemical array was transmitted through a dichroic mirror and detected by a CCD camera (PXL-37, Photometrics, Tucson, AZ). The emission wavelength for $Ru(bpy)_3^{2+}$ is 670 nm. Images were collected every 500 ms for 400 ms either by scanning the potential from 0.8 to 1.3 V/Ag/AgCl (scan rate 0.02 V s^{-1}) or by applying a potential of 1.2 V/Ag/AgCl to the array.

SEM images were obtained with a field emission scanning electron microscope FE-SEM (LEO 982, Thornwood, NY) located at Harvard University.

Electroless Gold Deposition. Gold nanoparticles were deposited around the surface of individual optical glass fibers (diameter 25 μm) using an electroless deposition method similar to that described by Martin.[19] About 600 individual fibers, which were held together on one side with a rubber tube, were immersed into "piranha solution" (70% H_2SO_4, 30% H_2O_2), rinsed with water and methanol, and dried (Caution: piranha solution reacts violently with organic materials). These cleaned fibers were then immersed for 20 min into a solution of 0.026 M $SnCl_2$ and 0.07 M trifluoroacetic acid in 50% v/v methanol/water. This procedure deposits the Sn^{2+} "sensitizer" onto the glass surface of the fibers. The fibers were rinsed with methanol thoroughly and immersed further into an aqueous solution of ammonical $AgNO_3$ (0.035 M) for 15 min leading to the deposition of silver nanoparticles on the fibers while oxidizing the surface-bound Sn^{2+} to Sn^{4+}. Following the deposition of silver, the fibers were rinsed with methanol and water. These silver-coated fibers were then immersed with stirring in an aqueous solution of 0.079 M $Na_3Au(SO_3)_2$, 0.127 M Na_2SO_3, and 0.625 M formaldehyde for 60 min in a water bath of 4 °C. Formaldehyde was oxidized catalytically by the silver particles and gold was reduced concurrently to elemental gold and deposited on the fiber surface. After the fibers were coated with gold, they were rinsed thoroughly with water and immersed overnight into 25% nitric acid solution to dissolve residual Ag and Sn particles exposed on the surface of the fiber. The gold-covered fiber was then rinsed with methanol and water and dried. The final product was dark red to golden yellow, depending on the thickness of the gold coating.

A self-assembled monolayer was deposited on the surface of the gold-coated fibers by immersing the fibers into ethanolic solutions containing 10 mM 11-mercapto-1-undecanol. This step was done to prevent each fiber from being in electrical contact with others. These insulated fibers were dipped into an epoxy polymer, which was cured at 100 °C in the oven for several hours. The coating was necessary so that the distal end of the fibers could be polished. It also ensured total light reflection in the fiber. Out of the total of 600 optoelectrodes, 20−30% were electrically wired to a copper wire through a silver paste. This procedure helped to minimize diffusional overlap at longer times.

(23) Bronk, K. S.; Michael, K. L.; Pantano, P.; Walt, D. R. *Anal. Chem.* **1995**, *67*, 2750.

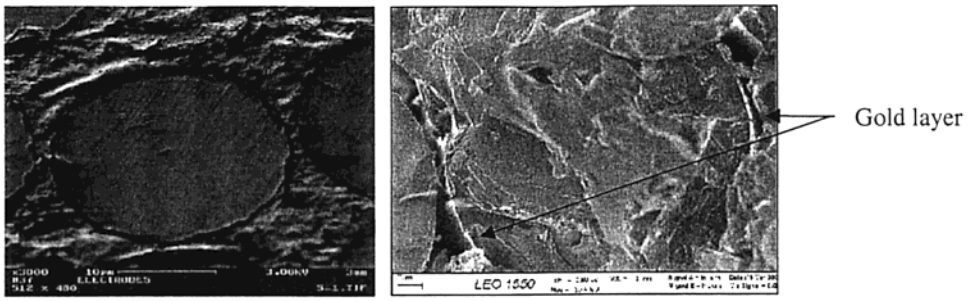

Figure 1. FE-SEM images of (A) part of the optoelectrochemical microring array based on optical fibers (diameter 25 μm) embedded in the epoxy layer and (B) the outer gold layer.

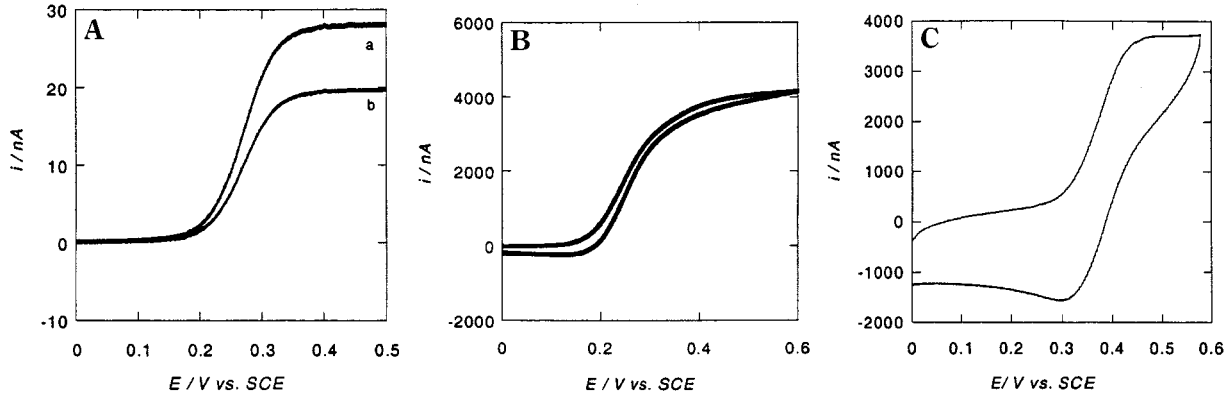

Figure 2. Cyclic voltammogram of (A) disk electrode 25-μm diameter (a) and fiber/gold ring electrode (b), (B) microarray with SAM, and (C) microarray without SAM. Solution, 10 mM $Fe(CN)_6^{4-}$/0.1 M KCl; scan rate, 0.01 V s^{-1}.

RESULTS AND DISCUSSION

The 600 individual optical fibers (diameter 25 μm) of 10-cm length were bundled at one end and coated simultaneously with gold via an electroless deposition procedure. These gold-coated fibers were covered with a thiol layer to insulate each fiber from its neighbors. The fibers were embedded in an insulating polymer and the distal end of the resulting array was polished, thus exposing gold-ring microelectrodes. About 20−30% of these ring electrodes were connected to an electrical wire. This array of microring electrodes was characterized using FE-SEM. Cyclic voltammetry and chronoamperometry were performed to characterize the electrochemical behavior of the microring array. Finally, the array was examined for its applicability to spectroelectrochemical problems.

SEM. Figure 1A shows a FE-SEM of some fiber electrodes of the random assembly embedded in the epoxy structure. The fibers are totally insulated from their neighbors by the epoxy layer. The center-to-center distance of the fibers is between 30 and 100 μm. FE-SEM was further used to visualize the gold layer around the ring. As the optical fibers are not conducting, charging effects are seen in Figure 1B. The gold ring is seen as the bright region around the optical fiber (see arrows in Figure 1B) and its thickness is estimated as being roughly 300 nm.

Cyclic Voltammogram. When designing random assemblies of electrodes, it is important to avoid diffusional interference between adjacent electroactive areas. A careful design is needed if an assembly of microring electrodes is to show steady-state currents that are several times larger than a single microelectrode. Fletcher[20] has suggested that for diffusion to be neglected, the ratio of the interelectrode distance d to the radius of the electrode r has to be $d/r \geq 20$. In our case, using an optical fiber of $r = 12.5$ μm, an average spacing between the microrings greater than 250 μm would be required. Such a device, based on the electroless deposition of gold around optical fibers, was formed by connecting only 20−30% of the 600 gold-covered fibers in the bundle. This procedure enabled the individual rings to be spaced by ~250 μm, so that interferences due to diffusional overlap would be minimized.

Steady-state current potential curves were recorded, which enables the determination of the number of active electrodes in the array and allows us to obtain some indication about the spacing between electrodes. Figure 2A shows cyclic voltammograms of a disk electrode ($r = 12.5$ μm) and a gold particle-coated single fiber ($r = 12.5$ μm + 0.3-μm gold) polished on its end to expose a microring electrode. The microring fiber/electrode shows a sigmoidal waveform at slow scan rates. An initial estimate of the size of the electrode ring can be made by measuring the steady-state current i_{disk} recorded with a disk microelectrode of the same outer radius b through its steady-state current (eq 1)

$$i_{disk} = 4nFD_{Fe(II)}c_{Fe(II)}b \quad (1)$$

where n is the number of electrons, F is the Faraday constant, D is the diffusion coefficient ($D_{Fe(II)} = 6.0 \times 10^{-6}$ cm s^{-1}), c is the

concentration of the electroactive species ($c = 10$ mM), and b is the outer ring radius ($b = 12.8$ μm), respectively.

According to Ewing,[24] the limiting steady-state current of a ring can be predicted from the current of a disk electrode of equal radius. Taking account of the 300-nm gold layer around the fiber ($b = r_{fiber}$+300-nm gold), the outer radius of the ring/fiber is $b =$ 12.8 μm and the current should reach a plateau at 2.96×10^{-8} A for a disk electrode. As seen in Figure 2A, however, the current recorded on the microring is slightly lower compared to a disk electrode with the same outer radius. The numerical difference in steady-state current for the ring compared to the disk electrode is ~67%. Bard[13] showed that, for a ratio of inner radius/outer radius $a/b = 0.97$, the ring current is only 68% of the disk, a value that compares nicely with our ring electrode. Therefore, a ring disk-shaped electrode with inner radius a and outer radius b should result in 33% smaller currents than a comparable disk electrode with the same radius b.

The current of a single gold-coated fiber ring was used as a reference for estimating the number of active rings in the high-density array. Ideally an array of N microelectrodes should yield a current amplification relative to a single electrode by a factor of N, where N is the number of active electrodes in the array.[25]

$$i_{array} = N i_{micro} \tag{2}$$

In practice, these expectations are fulfilled only if certain very strict requirements concerning the array design are met. If the electrodes are too closely packed, their diffusion layers will overlap and the current response approaches that of a macroelectrode.

Figure 2B shows the voltammogram of the microelectrode array in a 10 mM aqueous solution of ferrocyanide. The steady-state current responses were preserved in this array format and give a useful qualitative indication that the spacing between the active ring sites is sufficient such that the diffusion fields do not overlap. Some overlap of diffusion layers may still take place as the arrangement of the electrodes and its connection was random and proved to be difficult to control. Depending on the particular array, some areas of the device have electrodes that are clustered, while in other parts, the distance for nondiffusional overlap is observed entirely. Furthermore, if two fibers touch each other, we would still observe microelectrode behavior with steady-state currents, as the final diameter of these ring fiber electrodes would be 50 μm. As there are ~200 ring electrodes in the array, the error in the steady-state current should be minimal. The limiting current was used as an indication and a first approximation of the number of active sites on the array. The number of active sites N is estimated by dividing the limiting current of the array by the limiting current for a single fiber electrode (Figure 2A) performed under the same conditions. Using this assumption, we estimate that ~200 microring electrodes were active.

As discussed above, the CV shows the characteristic shape for spherical and nonplanar diffusion at microelectrodes and suggests that the majority of the fibers are separated and that the diffusion layers do not overlap significantly. If the interelectrode spacing was not large enough, a characteristic macroelectrode-shaped CV peak would have been observed. It is important to emphasize that the SAM layer was essential to obtaining these steady-state results. Figure 2C shows the CV of an assembly where the gold-deposited array was only sealed into epoxy. As seen in the figure, the current height of the device is the same, but instead of an expected steady-state current, a peak-shaped CV was observed. This result can be explained by the fact that some of the fibers were in close contact, leading to a characteristic macroelectrode response.

Chronoamperometry. To verify the assumption that large spacing between the individual rings exists, chronomamperometric measurements were undertaken. The current versus time dependency of a microring electrode can be considered as a limiting case of a band at short times and a disk microelectrode at longer times. The current on a microdisk and a microring electrode can approach a steady-state value while the current on a band microelectrode decays with the reciprocal logarithm of time. Similar to a band electrode, the ring microelectrode has a higher perimeter-to-area ratio than the disk microelectrode. Many contributions have been devoted to developing a theory of the diffusion-controlled steady-state current $\lim i(t)$ of bands and disks. The steady-state behavior for a ring electrode was described by Szabo[26] and Fleischmann,[27] where $\lim i(t)$ was calculated by assuming uniform accessibility to the surface of the ring electrode of arbitrary thickness. According to Szabo,[26] the limiting current at time t at a microring is given by

$$\lim i(t) = nFDcl_0[1 + l_0/(4\pi^2 Dt)^{1/2}] \tag{3}$$

$$l_0 = [\pi^2(a + b)/\ln[32a/(b - a) + \exp(\pi^2/4)]$$

where a is the inner ring radius and b is the outer ring radius, respectively. This treatment assumes that the insulating sheet is infinitely thick and a uniform flux to the surface of the electrode is maintained.

Chronoamperometric curves of one of the optical fibers coated with gold nanoparticles were recorded in 10 mM aqueous ferrocyanide solutions for times up to 5 s (Figure 3A). The experimental data shown in Figure 3A (points) are in good agreement with the theoretically calculated ones (line) using eq 3 with the respective variables being: $D_{Fe(II)} = 6.0 \times 10^{-6}$ cm s^{-1}, $c = 10$ mM, $a = 12.5$ μm, and $b = 12.8$ μm. In the case of a microring array, the chronomamperometric response depends on the time frame of the experiment. At short times, where each individual ring is separated and no interference from overlapping diffusion is expected if the interelectrode distance is sufficiently large, the current decay should be $1/\sqrt{(t)}$, as described by Szabo,[26] and show Cotrellian behavior. From the chronoamperometric signal of the array in Figure 3B, this value seems to be indeed the case if we assume we have 200 individual active electrodes and multiply the limiting current by this factor. At longer times, a more complex behavior is expected, changing from Cotrellian to cylindrical diffusion behavior ($1/\ln t$) and finally to planar diffusion of the whole array ($1/\sqrt{(t)}$,), resembling a macroelectrode.

If we assume the thickness of the microring to be 300 nm, the typical time expected to reach steady-state current is on the order

(24) Wallingford, R. A.; Ewing, A. G. *Anal. Chem.* **1988**, *60*, 1972.
(25) Morf, W. E. *Anal. Chim. Acta* **1996**, *330*, 139.
(26) Szabo, A. *J. Phys. Chem.* **1987**, *91*, 3108.
(27) Fleischmann, M.; Pons, S. *J. Electroanal. Chem.* **1987**, *222*, 107.

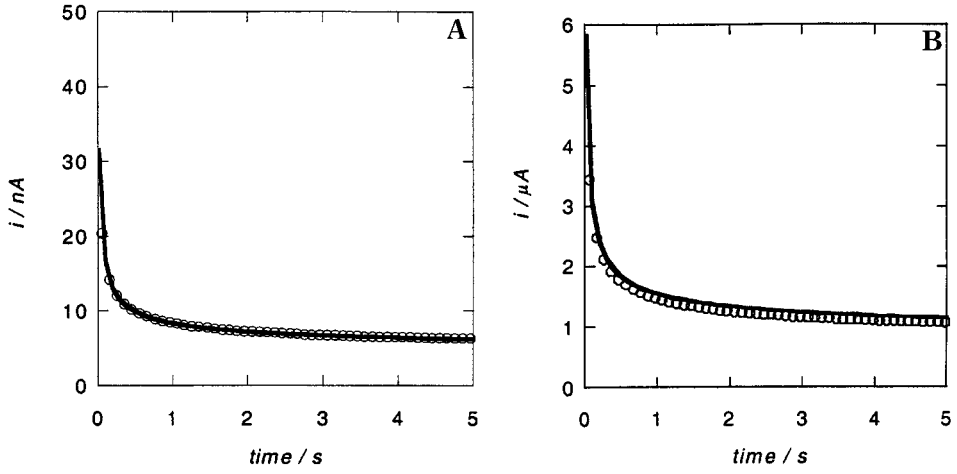

Figure 3. Comparison of the chronoamperometric current (dotted line) of (A) a single ring/fiber electrode and (B) microelectrode array with the limiting current predicted by Szabo. Solution, 10 mM $Fe(CN)_6^{4-}$/0.1 M KCl.

of l^2/D,[26] where l is the characteristic dimension of the electrode. In the case of a ring, l is taken as the inner radius a of the ring and the time calculated to reach steady-state behavior is 0.26 s, which is feasible taking into account that steady-state currents develop rapidly at microelectrodes. Taking eq 4 as an approxima-

$$\delta = \sqrt{(Dt)} \tag{4}$$

tion for the dimension of the diffusion layer developed on the ring, the thickness of δ will be 12 μm. This value corresponds to the inner radius a of the ring/fiber electrode.

At 5 s, δ would have grown to ~60 μm so that if the spacing between the electrodes is larger than 60 μm, no diffusional interferences and therefore no macroelectrode behavior will be observed, as shown in Figure 3B.

Electrogenerated Chemiluminescence. Electrochemical oxidation of $Ru(bpy)_3^{2+}$ results in chemiluminescence in the presence of TPrA. Novel spectroelectrochemical sensors embodying two modes of instrumental selectivity, electrochemical and spectroscopic, have been described by Heineman.[28] A critical review of the analytical applications of $Ru(bpy)_3^{2+}$ as a chemiluminescent reagent has recently been published.[29] The ECL of an electrolyte solution results from the electron-transfer reaction of ion radicals produced from an organic reactant that generates an excited-state product and luminesces when it relaxes to its ground state. The ECL intensity is a quantitative characteristic of the rate of such an electron-transfer reaction.

We have used the aqueous system of $Ru(bpy)_3^{2+}$/TPrA to demonstrate that the microring optical fiber array can be used for the detection of light. The electrogenerated chemiluminescence (ECL) mechanism of this system has been intensively investigated.[30] At high concentrations of $Ru(bpy)_3^{2+}$ (>0.1 mM), the catalytic oxidation of TPrA by electrogenerated $Ru(bpy)_3^{3+}$ is the dominant process of ECL as described by the following equations:

$$Ru(bpy)_3^{2+} \rightarrow Ru(bpy)_3^{3+} + e \qquad E^0 = 1.26 \text{ V/SCE} \tag{5}$$

$$Ru(bpy)_3^{3+} + TPrA \rightarrow Ru(bpy)_3^{2+} + TPrA^+ \tag{6}$$

$$TPrA^+ \rightarrow TPrA^\bullet + H^+ \tag{7}$$

$$Ru(bpy)_3^{3+} + TPrA^\bullet \rightarrow Ru(bpy)_3^{2+*} + \text{products} \tag{8}$$

$$Ru(bpy)_3^{2+*} \rightarrow Ru(bpy)_3^{2+} + h\nu \tag{9}$$

To perform ECL, the assembly was placed into a voltammetric cell, comprising a 1-mL volume. A platinum plate counter electrode was placed parallel to the device. This positioning ensured that no reflected light from the platinum surface would be collected by the optical fibers.[11] We performed ECL by stepping the potential from 0.80 V/Ag/AgCl, where no electrochemical reaction takes place, to 1.30 V/Ag/AgCl where oxidation of $Ru(bpy)_3^{2+}$ and the catalytic oxidation of TPrA occurs (Figure 4). The ECL intensity increased rapidly at a potential more positive than 1.0 V, reaching a constant level from 1.1 to 1.30 V/Ag/AgCl. Light was collected at 550−650 nm, the emission region of the $Ru(bpy)_3^{2+}$. When the potential was held constant at 1.30 V/Ag/AgCl, ECL emission increases via an initial fast rise occurring at time constants on the order of 0.23 s, followed by a comparatively slow increase to the steady-state limit. In this manner, the electrochemical properties of the ring and its ability to collect light with the same device were demonstrated.

The analytical utility of the chemiluminescence of $Ru(bpy)_3^{2+}$ depends on the emission of light, which is indicative of the concentration of the analyte in solution. The microarray was therefore exposed to different $Ru(bpy)_3^{2+}$ concentrations. Figure 5 shows a calibration curve for the ruthenium system using the microarray. To obtain reproducible signals, after each trial, the electrode was cleaned by pulsing it several times to remove any adsorbed or deposited materials.

(28) Gao, L.; Seliskar, C. J.; Heineman, W. R. *Electroanalysis* **2001**, *13*, 613.
(29) Gerardi, R. D.; Barnett, N. W.; Lewis, S. W. *Anal. Chim. Acta* **1999**, *378*, 1.
(30) Zu, Y.; Ding, Z.; Zhou, J.; Lee, Y.; Bard, A. *J. Anal. Chem.* **2001**, *73*, 2153.

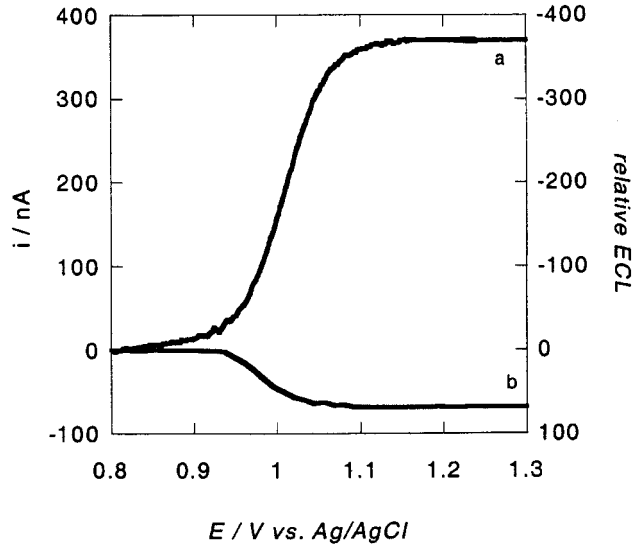

Figure 4. Development of ECL intensity on an optoelectrochemical microarray: (a) voltammogram and (b) corresponding ECL curve; scan rate, 2 mV s^{-1}; solution, 1 mM $Ru(bpy)_3^{2+}$/0.1 M TPrA/0.15 M phosphate buffer (pH 7).

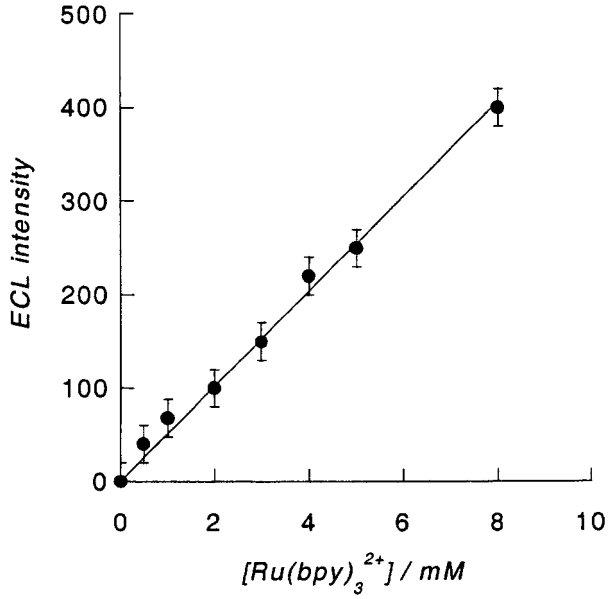

Figure 5. Calibration curve for ECL using the microarray: E_{app} = 1.2 V/Ag/AgCl; solution, x mM $Ru(bpy)_3^{2+}$/0.1 M TPrA/0.15 M phosphate buffer (pH 7). Each point is an average of five trials.

CONCLUSION

A novel optoelectrochemical device has been fabricated and demonstrated for concurrent electrochemical and optical measurements. The device comprises optical fibers coated with gold and assembled in a random array format. The array was electrochemically characterized by CV and chronoamperometry. The design yielded an array of ~200 microring electrodes, where interdiffusional problems were minimized. This device was then used to demonstrate that electrochemically generated luminescent products can be detected with the fiber assembly. This device has the potential to be used as an optoelectronic sensor, especially for the electrolytic generation and transmission of electrochemiluminescence. It is important to point out that while all the fibers are optically addressable, not every fiber is electrochemically addressable. The resolution of this device is in the tens of micrometers range, determined by the diameter of the optical fiber (25 μm) and by the spacing between each electrically connected fiber. For the purpose of having well-behaved microelectrode characteristics, this spacing was designed to be larger than 60 μm. To overcome this limitation, the construction of an ordered optelectrochemical device is underway in our laboratory and should allow chemical and electrochemical sensing as well as imaging of surfaces with good spatial resolution.

ACKNOWLEDGMENT

The authors thank Yuan Lu and Jenny Tam for help with SEM measurements and the National Institutes of Health for financial support.

Received for review August 21, 2001. Accepted December 3, 2001.

AC010933T